Acta Crystallographica Section D
Biological Crystallography
ISSN 0907-4449

A plant-seed inhibitor of two classes of α-amylases: X-ray analysis of *Tenebrio molitor* larvae α-amylase in complex with the bean *Phaseolus vulgaris* inhibitor

Virginie Nahoum,[a] Francesca Farisei,[b] Véronique Le-Berre-Anton,[c] Marie P. Egloff,[a] Pierre Rougé,[c] Elia Poerio[b] and Françoise Payan[a]*

[a]AFMB-IBSM-CNRS, 31 Chemin Joseph Aiguier, 13402 Marseille CEDEX 20, France, [b]Dipartimento di Agrobiologia e Agrochimica, Universita' della Tuscia, via S. Camillo De Lellis, 01100 Viterbo, Italy, and [c]Institut de Pharmacologie et de Biologie Structurale, UPR 9062, 205 Route de Narbonne, 31077 Toulouse CEDEX, France

Correspondence e-mail: payan@afmb.cnrs-mrs.fr

Received 27 May 1998
Accepted 4 August 1998

The α-amylase from *Tenebrio molitor* larvae (TMA) has been crystallized in complex with the α-amylase inhibitor (α-AI) from the bean *Phaseolus vulgaris*. A molecular-replacement solution of the structure was obtained using the refined pig pancreatic α-amylase (PPA) and α-AI atomic coordinates as starting models. The structural analysis showed that although TMA has the typical structure common to α-amylases, large deviations from the mammalian α-amylase models occur in the loops. Despite these differences in the interacting loops, the bean inhibitor is still able to inhibit both the insect and mammalian α-amylase.

1. Introduction

α-Amylase (α-1,4 glucan-4-glucanohydrolase, E.C. 3.2.1.1) catalyses the hydrolysis of α-(1,4) glycosidic linkages of starch components. *Tenebrio molitor* (yellow mealworm) is one of the most common pests responsible for damaging grain and stored crops; these insects cause enormous losses during food-stuff storage. The complete amino-acid sequence of the *T. molitor* α-amylase (TMA; 51.3 kDa, 471 amino-acid residues) was recently determined (Strobl *et al.*, 1997) and found to show a sequence identity of 54% to pig pancreatic α-amylase (PPA). TMA is inhibited by a protein (α-AI) isolated from the common bean *Phaseolus vulgaris* (Powers & Culberston, 1983).

α-AI is a plant-defence protein and a potent inhibitor of both mammalian and insect α-amylases (Powers & Whitaker, 1977). Understanding the mode of action of these proteins against the two classes of enzymes at the molecular level may provide insights into the main rules underlying their inhibition process. We recently solved the structure of two mammalian α-amylases (PPA and HPA) in complex with α-AI (Bompard-Gilles *et al.*, 1996; V. Nahoum *et al.*, unpublished results). Here, we report on the structure of an insect α-amylase in complex with the bean inhibitor; the present study shows how insect α-amylases and mammalian α-amylases may recognize the same proteinaceous inhibitor.

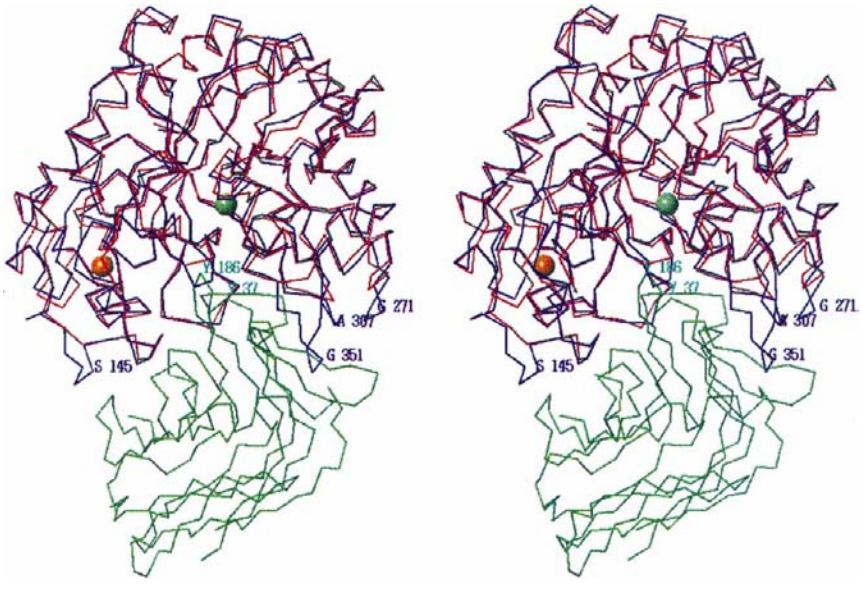

Figure 1
A stereoview of the superimposed Cα backbone traces of TMA (red) and PPA (blue) regions interacting with α-AI (one monomer; green). The yellow and green spheres indicate the calcium and chloride ions present in the TMA structure, respectively.

2. Materials and methods

2.1. Purification and crystallization.

TMA and α-AI were purified as previously described (Buonocore *et al.*, 1975; Le-Berre *et al.*, 1997). The lyophilized proteins TMA and α-AI were rehydrated to concentrations of 10 mg ml^{-1}, mixed together stoichiometrically and incubated at room temperature for 1 h. The crystallization trials were carried out using the hanging-drop vapour-diffusion method (McPherson, 1982). Single crystals suitable for X-ray analysis (0.2 × 0.1 × 0.03 mm) were obtained after 2 d at room temperature in drops consisting of 1 µl of enzyme-complex solution and 1 µl reservoir solution containing 0.1 *M* sodium cacodylate (pH 7), 13% PEG 6000 and 1 *M* $MgCl_2$.

2.2. X-ray diffraction pattern.

A 3.0 Å data set was collected at 100 K at the beamline DW32 (LURE, Paris) using cryocooling conditions. A total of 161 frames (1° oscillation) were collected from one crystal

Table 1
Data-collection and refinement statistics.

Resolution range 10–3.0 Å. Data statistics for the last shell (3.1–3.0 Å) are given in parentheses.

Cell parameters (*C*2)	
a (Å)	168.475
b (Å)	75.911
c (Å)	61.989
β (°)	101.290
Resolution limit (Å)	3.00
Number of measurements	45403 (4420)
Unique reflections	14982 (1499)
Data >1σ (%)	88.5 (70.4)
Completeness	99.3 (99.3)
Average multiplicity	3.0 (2.9)
$R_{\rm merge}$†	0.153 (0.450)
$I/\sigma(I)$	4.1 (1.3)
B value from Wilson plot (Å^2)	38.1
Refinement range (Å) (with bulk solvent correction)	10–3.0
Number of reflections in refinement ($F > 1\sigma_F$)	14976
R factor‡	0.230
$R_{\rm free}$	0.291
Number of protein atoms	5162
Group *B* factor	
Main chain (Å^2)	33.5
Side chain (Å^2)	36.9
R.m.s. deviations	
Bond lengths (Å)	0.020
Angles (°)	2.102
Estimated coordinate error from Luzzati plot (Luzzati, 1952) (Å)	0.55

† $R_{\rm merge} = \sum_h \sum_i |I_{h,i} - \langle I_h \rangle| / \sum_h \sum_i |I_{h,i}|$. ‡ The crystallographic *R* is defined as $\sum |F_o - F_c| / \sum |F_o|$; $R_{\rm free}$ is calculated in the same way on a subset of reflections which are not used in the refinement; F_o and F_c are the observed and calculated structure factors, respectively.

on a 300 mm MAR Research imaging plate. The data were processed with the *DENZO* and *SCALEPACK* programs (Otwinowski & Minor, 1997). Data-collection statistics are given in Table 1.

3. Results and discussion

The molecular-replacement calculations were performed in the 8–4 Å resolution range using the *AMoRe* program suite (Navaza, 1994). The rotation search gave unique solutions for the enzyme (peak height 22.0) and for the inhibitor (peak height 23.2). The enzyme gave the best translation-function solution with a correlation coefficient (CC) of 0.376 and an *R* factor (R_f) of 0.461 (second solution: CC = 0.258, R_f = 0.503). This yielded a unique phased translation-function solution (CC = 0.559 and R_f = 0.393). The CC and R_f values were improved to 0.686 and 0.326, respectively, after rigid-body refinement. The process yielded an E_2I_2 complex model consistent with good packing and two EI (enzyme/inhibitor) entities linked by the twofold crystallographic axis. One monomer (EI) in the asymetric unit results in a V_m value (Matthews, 1968) of 2.6 Å^3 Da^{-1} and a solvent content of 53%. The electron-density maps calculated at this stage were sufficiently clear to be able to incorporate the TMA sequence. After the first cycle of the refinement procedure using the program *X-PLOR* (Brünger, 1996), the *R* value was 0.287 and the $R_{\rm free}$ value was 0.331. Alternating model rebuilding and simulated-annealing refinement cycles resulted in a 3.0 Å model with an *R* factor of 0.231 ($R_{\rm free}$ = 0.291). Details of the refinement and model statistics are listed in Table 1. At the 1σ level of the final $(2F_o - F_c)\exp(i\alpha_c)$ map, the TMA structure showed clearly defined patterns of density. Most of the side chains showed a clear-cut electron-density pattern, except for a few residues which had a weak density (residues 458 and 374–375) and were located in external loops (notation according to PPA). It should be noted that all the TMA residues involved in the interaction with inhibitor elements were perfectly defined. The quality of the model was assessed using *PROCHECK* (Laskowski *et al.*, 1993). Fig. 2(*a*) shows the Ramachandran plot (Ramakrishnan & Ramachandran, 1965) of the final model. The model clearly showed that the structures of PPA and TMA are homologous (Fig. 1). The chloride and calcium binding sites identified in the TMA–α-AI structure were identical to those observed in the PPA structure. All the most important residues (Qian *et al.*, 1994) involved in the catalysis and substrate binding occur in identical positions in the insect and mammalian α-amylases (Fig. 2*b*). The only exception is the residue His305, which participates strongly in the substrate binding and structural changes within the active site of mammalian enzymes. This residue is not conserved in TMA. Nevertheless, our results suggest that in the TMA–α-AI structure, the residue Thr307 makes a similar contribution to that of His305. The model consisting of TMA bound to α-AI shows deviations from the search model (PPA) because of the amino-acid deletions occurring in the long loops of the enzyme. Our previous structural analysis of PPA in complex with α-AI showed that three loops of the enzyme are involved in the interaction, namely the 'flexible loop'

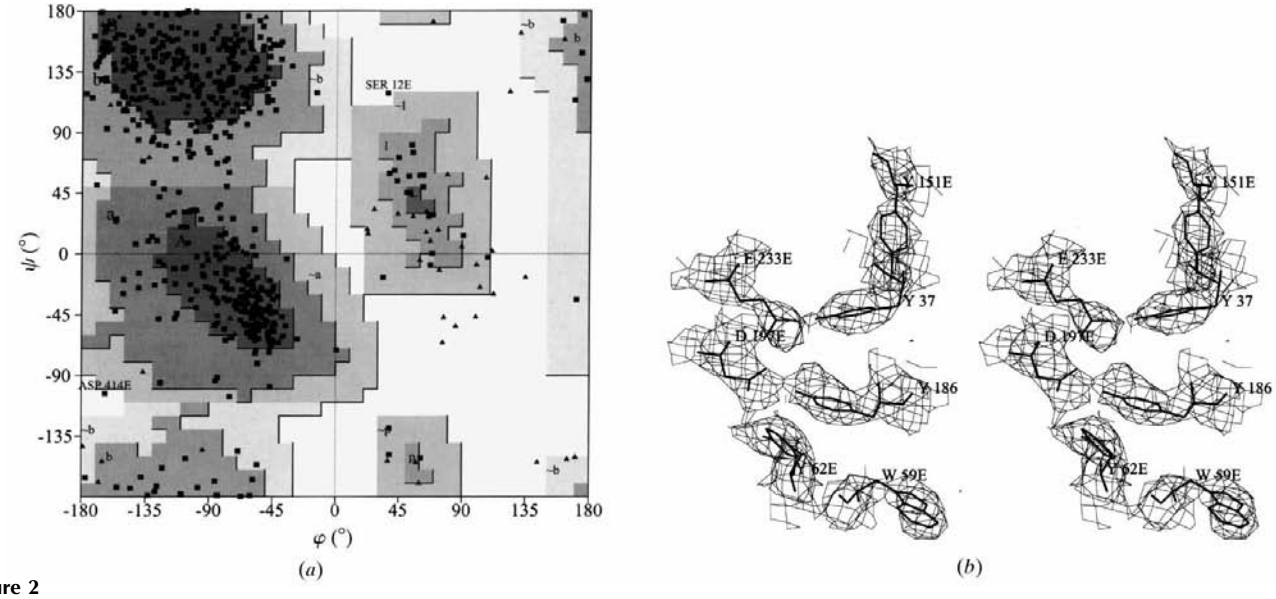

Figure 2
(*a*) Ramachandran plot for the final model of TMA/α-AI. (*b*) Stereoview of the electron-density map $(2F_o - F_c)\exp(i\alpha_c)$ (1σ level) in the active-site cleft of TMA. The enzyme residue numbers (numbering according to PPA) are followed by an 'E'.

within the active site (residues 303–312), the loop at position 347–354 and loop 140–150 originating from the meandrous loop inserted into the typical $(\beta/\alpha)_8$ barrel. It is worth noting that all three loops are severely truncated in the insect α-amylase. However, the interaction with the inhibitor is highly conserved. The two hairpin loops of the inhibitor (residues 29–46 and 171–189), which insert into the active site of the enzyme, establish a similar network of hydrogen bonds with the residues of the substrate-docking region to that observed in the PPA complex. The catalytic residues are strongly hydrogen-bonded to the inhibitor residues Tyr186 and Tyr37, which project into the heart of the catalytic site, and to the flanking residue Asp38 which occupies the reducing-end subsite. The 'flexible loop' which forms the surface edge of the binding cleft in the mammalian α-amylases still interacts with the inhibitor despite its shortened length. The interactions with the proteinaceous inhibitor involve only the extremities of the 'flexible loop' and, since these regions remain unchanged in the TMA structure, the hydrogen bonding with the inhibitor residues in this region is conserved. The enzyme convex loop (138–150, from the 'meandrous loop') interacting with the facing concave region of α-AI is truncated in TMA (residues 140 and 144–148 are deleted). However, the same number of enzyme residues is involved in the binding segment occurring in this part of TMA and the two direct hydrogen bonds passing through the main-chain carbonyl of residue Asn149 and hydroxyl side-chain group of Tyr151 (with inhibitor residues Ser78 and Asp38) are preserved. Slight changes occur in the interaction between the loop region located in the neighbourhood of the active site (residues 351–359) and the inhibitor. In the PPA–α-AI structure, this long loop forms a hydrogen bond with the inhibitor *via* residue 352. In the present model, although residues 346 to 355 are deleted, the interaction between this loop region of TMA and α-AI is maintained *via* neighbouring TMA residues 356 and 357.

It emerges clearly from the results of the present study that the strong contacts occurring in the catalytic cleft are highly conserved in both classes of enzymes. Although slight modifications occur in the extended protein–protein interaction, the partners manage to produce the same type of contacts in alternative ways.

References

Bompard-Gilles, C., Rousseau, P., Rougé, P. & Payan, F. (1996). *Structure*, **4**, 1441–1452.

Brünger, A. T. (1996). *X-PLOR Version 3.843 Manual.* New Haven, CT: Yale University Press.

Buonocore, V., Poerio, E., Gramenzi, F. & Silano, V. (1975). *J. Chromatogr.* **114**, 109–114.

Laskowski, R. A., MacArthur, M. W., Moss, D. S. & Thornton, J. M. (1993). *J. Appl. Cryst.* **26**, 283–291.

Le-Berre, V., Bompard-Gilles, C., Payan, F. & Rougé, P. (1997). *Biochim. Biophys. Acta*, **1343**, 31–40.

Luzzati, V. (1952). *Acta Cryst.* **5**, 802–810.

McPherson, A. (1982). *Preparation and Analysis of Protein Crystals*, pp. 82–127. New York: John Wiley.

Matthews, B. W. (1968). *J. Mol. Biol.* **33**, 491–497.

Navaza, J. (1994). *Acta Cryst.* A**50**, 157–163.

Otwinowski, Z. & Minor, W. (1997). *Methods Enzymol.* **276**, 307–327.

Powers, J. R. & Culberston, J. D. (1983). *Cereal Chem.* **60**, 427–429.

Powers, J. R. & Whitaker, J. R. (1977). *J. Food Biochem.* **1**, 217–238.

Qian, M., Haser, R., Buisson, G., Duée, E. & Payan, F. (1994). *Biochemistry*, **33**, 6284–6294.

Ramakrishnan, C. & Ramachandran, G. N. (1965). *Biophys. J.* **5**, 909–933.

Strobl, S., Gomis-Rüth, F.-X., Maskos, K., Frank, G., Huber, R. & Glockshuber, R. (1997). *FEBS Lett.* **409**, 109–114.